1-[Carbon-11]-Glucose Radiation Dosimetry and Distribution in Human Imaging Studies

Michael M. Graham, Lanell M. Peterson, Mark Muzi, Brian B. Graham, Alexander M. Spence, Jeanne M. Link and Kenneth A. Krohn

Departments of Radiology, Radiation Oncology and Neurology, University of Washington School of Medicine, Seattle, Washington

1-[Carbon-11]-D-glucose ([^{11}C]-glucose) is an important imaging agent for PET studies that have been used to study the normal brain, encephalitis, epilepsy, manic-depressive disorder, schizophrenia and brain tumors. **Methods:** Dosimetry estimates were calculated in subjects undergoing imaging studies to help define the radiation risk of [^{11}C]-glucose PET imaging. Time-dependent radioactivity concentrations in normal tissues in 33 subjects after intravenous injection of [^{11}C]-glucose were obtained by PET imaging. Radiation absorbed doses were calculated according to the procedures of the Medical Internal Radiation Dose (MIRD) committee along with the variation in dose based on the calculated standard deviation of activity distribution seen in the individual patients. **Results:** Total body exposure was a median of 3.0 μGy/MBq in men and 3.8 μGy/MBq in women. The effective dose equivalent was 3.8 μGy/MBq in men and 4.8 μGy/MBq in women. The critical organs were those that typically take up the most glucose (brain, heart wall and liver). **Conclusion:** The organ doses reported here are small and comparable to those associated with other commonly performed nuclear medicine tests and indicate that potential radiation risks associated with this radiotracer are within generally accepted limits.

Key Words: carbon-11; glucose; dosimetry; Monte-Carlo simulations

J Nucl Med 1998; 39:1805–1810

1-[Carbon-11]-glucose is a radiotracer that is taken up in areas of increased glucose metabolic activity. It has been used in the study of the normal brain (*1,2*), encephalitis (*3*), epilepsy (*4*), manic-depressive disorder (*5*), schizophrenia (*6–8*) and brain tumors (*9–11*).

Glucose is the main substrate for energy metabolism in the brain, and it is taken up and metabolized by every tissue in the body. Metabolism results in a wide variety of labeled products, primarily carbon dioxide and lactate, which may be released and circulate in the blood. The rate of metabolism and the distribution of labeled products depends to some extent on the location of the radioactive carbon in the molecule. The dosimetry studies reported here are for glucose labeled in the C-1 position. Dosimetry estimates for [^{11}C]-glucose labeled in other positions will probably be somewhat different than the values reported here. The only report of [^{11}C]-glucose dosimetry of which we are aware is by Powers (*12*). His estimates were based on blood time-activity curves and literature values of the tissue distribution of tracer glucose. In contrast, the study reported here is based on blood and tissue measurements with PET measurements of 1-[^{11}C]-glucose. This more direct approach yields dosimetry estimates that are quite different from those estimated by Powers.

Received Aug. 26, 1997; revision accepted Jan. 14, 1998.

For correspondence or reprints contact: Michael M. Graham, PhD, MD, Mail Stop 356113, Department of Radiology (Nuclear Medicine), University of Washington, Seattle, WA 98195.

MATERIALS AND METHODS

Human Subjects

Biodistribution data from 28 patients (16 men, 12 women) and 5 normal volunteers (3 men, 2 women) who had [^{11}C]-glucose PET scans at the University of Washington between October 1993 and April 1996 were used for dosimetry estimates. Fourteen patients (9 men, 5 women) had brain gliomas and 14 (7 men, 7 women) had abdominal tumors. The normal volunteers all received brain scans only. The median weight was 79 kg (range: 54–118 kg), height 174 cm (range: 155–185 cm) and age 48 yr (range: 21–76 yr). All patients fasted overnight before the PET study and all blood glucose levels were within the normal range (median: 5.3 m*M*, range 4.2–6.6 m*M*). The tissues imaged for dosimetry estimates were studied at sites distant from the source of primary pathology. All of these patients also received an injection of [^{18}F]-fluorodeoxyglucose approximately 90 min after the injection of [^{11}C]-glucose, but it was not used in this assessment of absorbed dose. The imaging procedure was approved by the institutional human subjects review committee and informed consent was obtained from all patients before imaging.

Carbon-11-Glucose

The synthesis of 1-[^{11}C]-D-glucose followed the method of Shiue and Wolf (*13*) as recently modified by Dence et al. (*14*) and by us (*15*). Typically, 1.7 Ci of [^{11}C] cyanide at end of bombardment yields 37 mCi 1-[^{11}C]-D-glucose. The glucose is separated from mannose and any other impurities using an Aminex HPX-87P 30 cm × 7.8 mm high-performance liquid chromatography column (BioRad Laboratories, Richmond, WA) at 70°C and eluted with sterile water. The radiochemical and chemical purity of the product was measured by analytical high-performance liquid chromatography using another Aminex HPX-87P column at 70°C eluted with deionized water and with refractive index and radioactivity detection of the effluent. Average radiochemical purity was > 98% with > 60 Ci/mmol specific activity. The radiopharmaceutical dose and the activity in a calibration vial were assayed in a dose calibrator (Capintec Model CRC-12, Montvale, NJ) before patient imaging.

Data Collection

All the patients were imaged with a GE Advance Positron Emission Tomograph (Waukesha, WI). The patients were positioned in the tomograph and an attenuation scan was obtained with a ^{68}Ge rotating sector source. Calibration vials were imaged separately from the patient and reconstructed using the same filter size as the emission images. The brain images were reconstructed with a filter size of 8 mm and the abdominal images were reconstructed with a filter size of 12 mm. Performance details for the tomograph have been reported (*16*).

Patients were injected with an average dose of 649 MBq (17.5 mCi) [^{11}C]-glucose and imaged. Blood samples were collected at selected intervals during the imaging procedure and counted in a 10-detector gamma well counter (Cobra; United Technologies

Packard, Chicago, IL). The multiple detectors in the gamma counter were normalized before each use with ^{68}Ge standards. Samples from the calibration vials were assayed also in the gamma counter to cross-reference between tomograph, gamma counter and dose calibrator. Glucose levels were determined from several blood samples during each study.

Most blood samples were arterial, collected with an automated blood sampler (*17*). The blood samples were decay corrected to the time the sample was drawn and scaled to units of Bq/g using the calibration factors determined above.

Calculation of Tissue Time-Activity Curves

The gamma counter calibration vial data were corrected for background and converted from cpm/g to Bq/g using the efficiency correction factors derived from standards that were measured using the dose calibrator. Tomograph images were reconstructed in intervals of 25 sec at the beginning of the study to 5 min at the end of the study. Regions-of-interest (ROIs) were drawn over the calibration vials of known Bq/g to determine efficiency. Data from each ROI for each time interval in cts/pixel were corrected for image duration and tomograph efficiency using data from the calibration vial, and converted to units of Bq/g. Lung activity was corrected using an average tissue density of 0.36 g/cm^3, previously calculated from the attenuation scans of a sample set of 18 patients using the approach described by Rhodes et al. (*18*). Tissue density in other organs was assumed to be 1 g/cm^3. The Bq/g values were then normalized to a 1-MBq injection in a 70-kg man or 1 MBq in a 57-kg woman. Total activity in each organ was calculated by assuming uniform distribution of activity throughout the organ and multiplying Bq/g by standard reference organ weights (*19*).

The normalized, not decay corrected, tissue activity (Bq/g) for each tissue for each patient was plotted against time (min), and fit by using the following empiric function:

$$\frac{Bq}{g} = A \cdot [t \cdot e^{-B \cdot t} + (1 - e^{-C \cdot t}) \cdot (D \cdot e^{-E \cdot t} + F \cdot e^{-G \cdot t})], \quad \text{Eq. 1}$$

using the "solver-add in" function in EXCEL 4.0 (Microsoft, Inc., Redmond, WA) to minimize the sum of the squares of the differences. This formula is a simple gamma variate with two exponentials in the tail used as a means to fit a curve so that it can be integrated; it is not an attempt to model the kinetics of [^{11}C]-glucose. Tissue data were not decay corrected since radiation exposure is proportional to the actual amount of activity present.

Radiation Dosimetry Calculation

The distribution of absorbed dose was calculated using S values obtained from MIRDOSE2 (*20*) according to the Medical Internal Radiation Dose (MIRD) scheme (*21*). Implicit to the MIRD scheme is the assumption that the integrated activity is known for each of the source organs. Observed source organs in this study included: brain, lung, heart wall, heart chamber, marrow, liver, spleen, kidney, lower large intestine, small intestine and upper large intestine combined, testes, ovaries, uterus and bladder. Source organ uptake varied between individuals, implying there was also a range of absorbed doses associated with the target organs. We estimated the range of absorbed doses to the target organs by using a Monte-Carlo simulation, repeating the following three steps 1000 times: (a) the integrated activity for each measured tissue was randomly chosen from the source organ data; (b) the dose to unobserved organs was calculated by assuming that all unaccounted activity was uniformly distributed throughout the body; and (c) the radiation doses to all target organs were calculated using S values according to the MIRD scheme. This scheme generated a distribution of expected radiation doses to the target organs. The process was done using a spreadsheet program (EXCEL 4.0; Microsoft, Inc., Redmond, WA) and a Monte-Carlo program (Crystal Ball 3.0; Decisioneering, Inc., Denver, CO). The approach is identical to that used in a previous study on ^{18}F-fluoromisonidazole dosimetry (*22*).

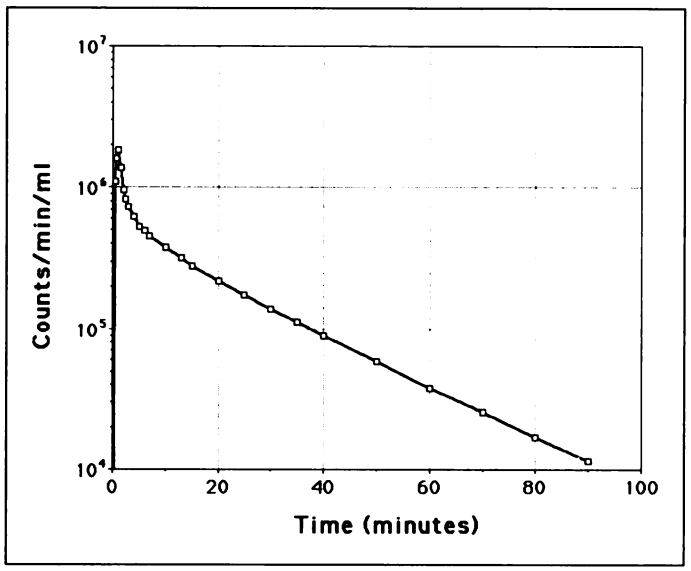

FIGURE 1. Semilogarithmic plot of a typical blood time-activity curve of ^{11}C activity after 1-min infusion of [^{11}C]-glucose. Subject was 27-yr-old woman with recurrent glioma. Samples were obtained using automated blood sampler.

Since there is no reported S value for brain to the lens of the eye, the value used was 4.3×10^{-5} rads/μCi hr or 1.2×10^{-5} Gy/MBq hr, based on the calculations described previously (*22*). Images of the head showed no excessive accumulation of activity in the area of the eye. The total dose to the lens was calculated using the above S value for brain along with the S values for thyroid as the target organ for all other sources. This approach should yield a slight overestimate of the radiation dose to the lens since the thyroid is somewhat closer to most of the source organs than the lens of the eye.

Effective dose equivalent to uniform whole-body exposure was determined by assuming a relative biological effectiveness of 1.0, and summing the product of appropriate organ weights (*23*) and the calculated dose estimates for each organ.

RESULTS

A typical blood time-activity curve, decay corrected to the time the samples were taken, is shown in Figure 1. There is an initial phase of equilibration lasting about 5 min, followed by exponential decrease in activity. Based on examination of curves from six subjects, the late phase has an effective half-life ($\pm$ s.d.) of 16.0 $\pm$ 0.4 min.

The tissue time-activity curves for the patient data for some of the source organs used are shown in Figures 2 and 3. The mean area under the curve ($\tilde{A}$) and standard deviation for each observed source organ, along with the number of patients and samples used, are shown in Table 1 for men and Table 2 for women.

The mean dose and the 25th and 75th percentiles for each organ are presented in Table 3 for men and Table 4 for women. The highest radiation absorbed doses are to the brain, heart wall and liver.

The calculated total body dose for an average 70-kg man injected with 1-[^{11}C]-glucose was 3.0 μGy/MBq. The calculated total body dose for an average 57-kg woman was 3.8 μGy/MBq. The effective dose equivalent was determined to be 3.8 μGy/MBq in men and 4.8 μGy/MBq in women.

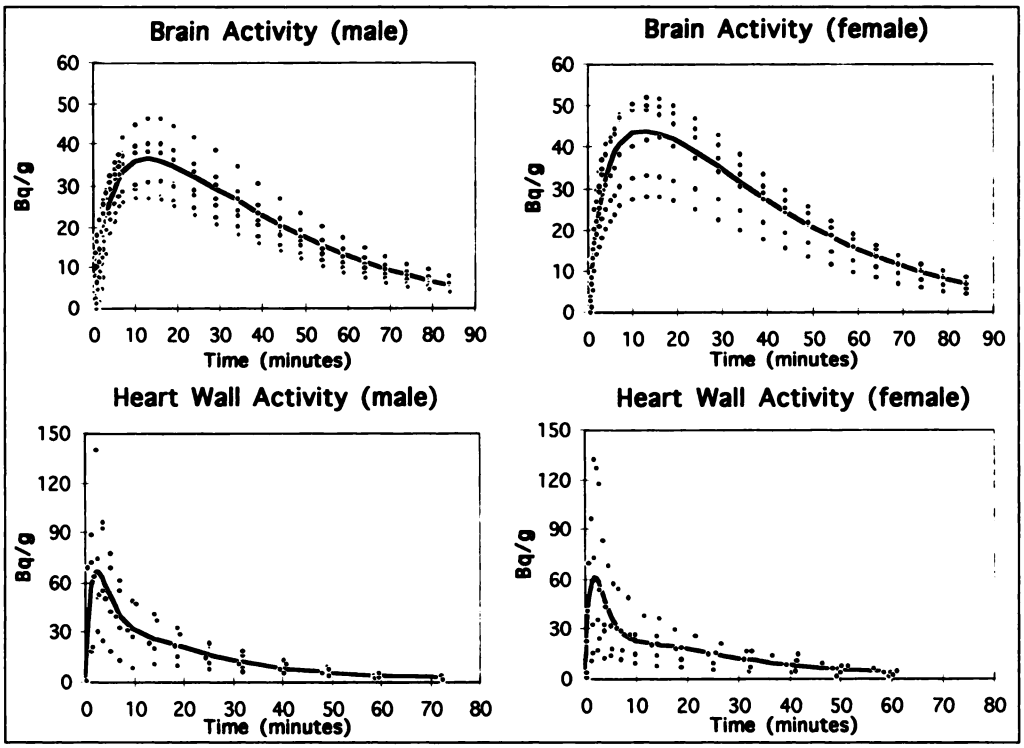

FIGURE 2. Activity of [^{11}C]-glucose in source organs, brain and heart wall, for both men and women. Data have been normalized to 1 MBq injected per 70 kg body weight for men and 57 kg body weight for women. Bold line is the fit of Equation 1 to the data.

DISCUSSION

1-[Carbon-11]-glucose shows substantial promise as an imaging marker for glucose metabolic rate in the normal brain (*1,2*), a wide range of diseases (*3–9,11*) and estimating the fluorodeoxyglucose (FDG) lumped constant (*10*). PET imaging of 1-[^{11}C]-glucose in patients with tumors indicates that this test can quantifiably detect increased uptake in tumors. When fully validated, this procedure may be used to calculate blood-to-brain glucose transport and true cerebral glucose metabolism. Because its use avoids any of the assumptions inherent with FDG, it is likely to find more widespread use in the future.

Glucose is inherently nontoxic and the dose used in patients for PET studies is well below a level that might cause chemotoxicity or other side effects. No adverse reactions were observed in this group of patients. This investigation concerned only the radiation exposure issues to better define the radiation risk of [^{11}C]-glucose PET imaging.

The only previous work on [^{11}C]-glucose dosimetry of which

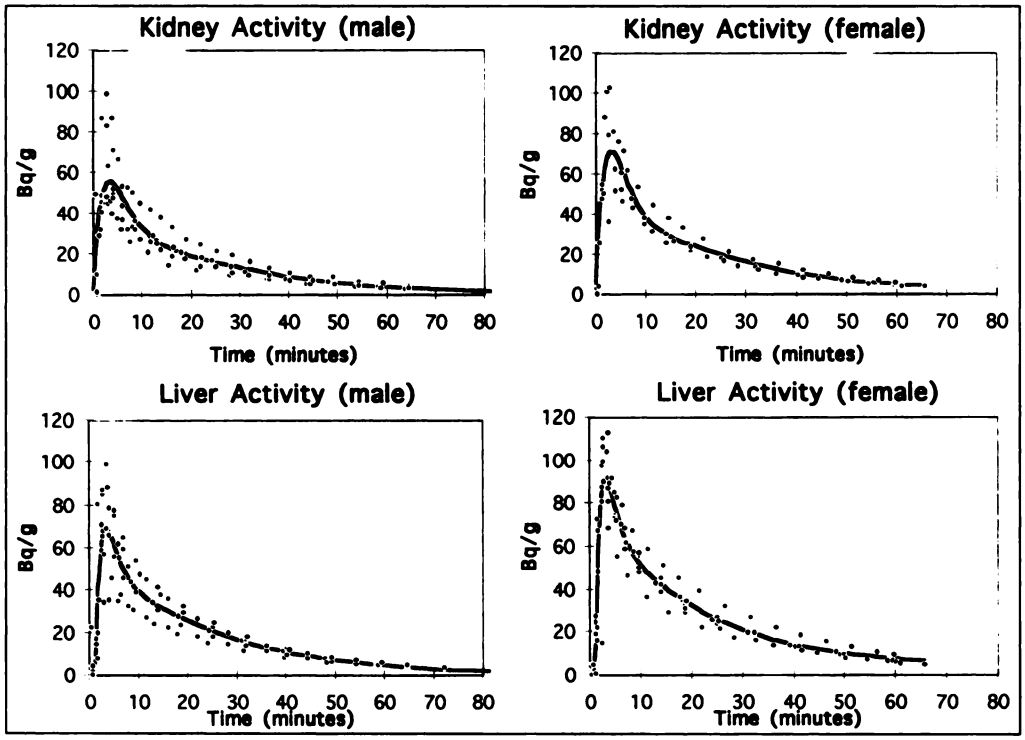

FIGURE 3. Activity of [^{11}C]-glucose in source organs, kidney and liver, for both men and women. Data have been normalized to 1 MBq injected per 70 kg body weight for men and 57 kg body weight for women. Bold line is the fit of Equation 1 to the data.

TABLE 1
Tissue Uptake of Carbon-11-Glucose in Males

Organ	Weight (g)*	Ã (kBq · hr/MBq)	± s.d.	No. of patients
Brain	1420	47.0	12.3	12 (308)
Lower large intestine	143	2.11	0.62	5 (69)
Gut (small intestine and upper large intestine)	655	9.45	2.19	7 (97)
Heart chamber (blood)	454	12.4	3.09	6 (85)
Heart wall	316	6.36	2.70	5 (71)
Kidneys	299	5.68	1.48	7 (99)
Liver	1910	46.0	10.9	7 (97)
Lungs	1000	14.0	2.80	6 (80)
Marrow	1120	10.2	1.67	7 (96)
Spleen	183	2.91	0.60	6 (81)
Testes	39	2.95	0.68	2 (28)
Bladder contents	211	0.89	0.56	5 (61)
Muscle	51800	198.9	35.4	7 (95)

*Weights are from Reference *19*.

we are aware is by Powers (*12*). His dosimetry estimates are based on blood time-activity curves from six human volunteers injected with randomly labeled [^{11}C]-glucose prepared through a photosynthetic route (*24*) and from six macaques injected with 1-[^{11}C]-glucose. Photosynthetic labeling results in the ^{11}C label distributed throughout the various positions of the glucose molecule. Metabolism is somewhat different depending on label location (*25*). C-3 and C-4 atoms are metabolized to CO_2 rapidly through the tricarboxylic acid (TCA) cycle, while C-1 and C-6 atoms must go through the TCA cycle 2.5 times before they are metabolized to CO_2. Atoms at the C-2 and C-5 positions have intermediate behavior, yielding CO_2 after 1.5 turns. Also when glucose enters the pentose cycle, the C-1 carbon is converted immediately to CO_2. These known different metabolic fates of the different labeling positions suggest the blood and tissue time-activity curves will be somewhat different for 1-[^{11}C]-glucose versus photosynthetically labeled glucose. The other reason our estimates are different than Powers' is that, in his approach, tissue activity was determined using published estimates. The resultant dosimetry estimates for most organs were considerably higher than were found in this study. Spleen, pancreas, lung, adrenal, thyroid, thymus, uterus and testes were higher by factors of 3–4. The total body estimated dose, however, was the same. Overall, the doses presented in Table 2 from this work are more realistic since most are within a factor of two of the whole-body dose and the target organs are those that are expected to have increased glucose uptake.

The results obtained in this study were checked to determine if they are plausible by a simple calculation. Assuming that 100% of the injected dose (1 MBq) was evenly distributed and retained throughout the body, the Ã for the total body should be:

$$1.0\text{MBq} \cdot \int_0^\infty e^{-(0.693 \cdot t/0.338)}\, dt = 0.488\text{MBq} \cdot \text{hr} \qquad \text{Eq. 2}$$

The half-life of ^{11}C is 0.338 hr.

Since the S value for the dose to the total body from the total body in 70-kg men is 5.84×10^{-6} Gy/MBq hr, the whole-body dose should be 2.84 μGy/MBq. For 57-kg women, the S value for dose to the total body from the total body is 7.32×10^{-6} Gy/MBq hr, making the whole-body dose 3.57 μGy/MBq. These conservative, average whole-body doses are comparable to the range of doses calculated for individual organs (0.9–11.0 μGy/MBq in men and 1.0–12.19 in women) and quite close to the calculated whole-body dose (3.0 and 3.8 μGy/MBq) (Tables 3 and 4).

Another test of the adequacy of the data is to check that the sum of the cumulative activity in all the measured organs accounts for most of the injected activity. The sum of the

TABLE 2
Tissue Uptake of Carbon-11-Glucose in Females

Organ	Weight (g)*	Ã (kBq · hr/MBq)	+/− s.d.	No. of patients
Brain	1410	52.2	18.6	9 (252)
Lower large intestine	109	2.18	0.37	6 (81)
Gut (small intestine and upper large intestine)	498	6.63	3.18	7 (103)
Heart chamber (blood)	347	12.2	4.06	5 (76)
Heart wall	241	3.88	1.99	5 (79)
Kidneys	248	5.62	0.99	4 (63)
Liver	1400	42.2	7.34	7 (107)
Lungs	651	18.5	1.44	4 (64)
Marrow	1050	9.72	2.63	7 (104)
Spleen	123	2.53	0.43	5 (76)
Ovaries	8.7	0.07	0.04	4 (55)
Uterus	79	1.42	0.19	3 (41)
Bladder contents	160	0.78	0.87	5 (63)
Muscle	40000	212.0	30.5	7 (102)

*Weights are from Reference *19*.

TABLE 3
Radiation Absorbed Dose to Male Organs for Administered Dose of 1.0 MBq

Target organ	Mean (μGy/MBq)	25th Percentile	75th Percentile
Adrenals	3.50	3.42	3.58
Brain	11.04	8.44	12.87
Gall bladder wall	3.19	3.05	3.33
Lower large intestine	3.34	2.92	3.89
Small intestine	3.26	2.92	3.68
Stomach	2.35	2.29	2.41
Upper large intestine	3.48	3.12	3.93
Heart wall	10.58	8.85	12.48
Kidney	6.56	5.66	8.12
Liver	8.72	6.74	10.12
Lungs	4.92	3.99	5.02
Muscle	2.78	2.70	2.86
Pancreas	3.57	3.48	3.65
Red marrow	4.21	3.94	4.48
Bone surface	2.89	2.84	2.95
Skin	0.87	0.86	0.88
Spleen	5.68	5.24	6.45
Testes	3.51	3.11	3.91
Thymus	3.07	2.99	3.15
Thyroid	3.82	3.43	4.21
Urinary bladder wall	2.00	1.65	2.23
Lens of eye	1.79	1.70	1.87
Total body	3.00	2.99	3.01

cumulative organ activity from Table 1 for men is 359 kBq hr and from Table 2 for women is 370 kBq hr. Compared to the expected cumulative activity of 488 kBq hr, this accounts for 74% in men and 76% in women. The unaccounted fraction was presumably distributed mostly in adipose tissue and other tissues not examined, with a small amount lost by expiration of carbon dioxide.

TABLE 4
Radiation Absorbed Dose to Female Organs for Administered Dose of 1.0 MBq

Target organ	Mean (μGy/MBq)	25th Percentile	75th Percentile
Adrenals	4.30	4.17	4.45
Brain	12.19	8.44	15.44
Breasts	2.99	2.88	3.10
Gall bladder wall	3.58	3.45	3.69
Lower large intestine	4.13	3.73	4.51
Small intestine	3.45	2.87	3.87
Stomach	2.78	2.69	2.88
Upper large intestine	3.50	2.87	3.97
Heart wall	11.00	9.43	13.00
Kidney	7.93	7.26	9.31
Liver	10.81	9.70	11.21
Lungs	8.92	9.06	9.46
Muscle	3.48	3.35	3.61
Ovaries	4.08	3.38	5.32
Pancreas	4.38	4.25	4.53
Red marrow	4.83	4.36	5.45
Bone surface	3.97	3.85	4.08
Skin	1.04	1.03	1.05
Spleen	7.22	6.63	7.23
Thymus	3.80	3.67	3.93
Thyroid	3.57	3.48	3.65
Urinary bladder wall	2.22	1.81	2.12
Uterus	6.58	5.96	6.96
Lens	2.22	2.11	2.32
Total body	3.82	3.80	3.84

The PET acquisition of [^{11}C]-glucose tissue time-activity curves provides data for the calculation of cumulative radiation doses to each organ that is accurate only within the counting limitations and spatial resolution of the tomograph. Thus dosimetry calculations of small, not visualized organs such as the adrenals were done assuming average total-body concentrations in those sites. Images that included these organs did not suggest any specific accumulation of activity.

In addition to the simplifications inherent in the MIRD phantom model (*21*), additional assumptions were made in the analysis of our data: (a) tracer distribution was assumed to be homogeneous throughout each organ; (b) tracer clearance was extrapolated after the last observed time point using the empiric formula (*1*), which is a good descriptor of the tisssue time-activity curves; (c) insulin levels were not measured, but none of the subjects was known to be diabetic and all had normal blood glucose levels ranging from 4.2–6.6 m*M*; and (d) the relatively wide range of activities seen in the various organs implies a relatively wide range of absorbed radiation doses. A Monte-Carlo simulation method was used to estimate this range.

The organ and total-body doses associated with [^{11}C]-glucose PET imaging are comparable to those associated with other widely used clinical nuclear medicine procedures. For example, the literature value for the effective dose equivalent for [^{18}F]-fluorodeoxyglucose is 24 μGy/MBq (*26*). This indicates that the radiation dose associated with an injection of 740 MBq (20 mCi) 1-[^{11}C]-glucose would be only about 40% of the dose received from 370 MBq (10 mCi) FDG.

CONCLUSION

To assess adequately a risk/benefits ratio, the actual benefits of a procedure must be well defined. Ongoing clinical trials assessing potential benefits of [^{11}C]-glucose PET imaging will establish its role in diagnosing and managing patients with various diseases. Should [^{11}C]-glucose PET imaging prove to be a useful clinical test, our current results indicate that radiation exposure resulting from the imaging procedure is at a reasonable risk level.

ACKNOWLEDGMENTS

We thank Barbara Lewellen and Nancy Bardon for their assistance with the studies. This work was supported by NIH grants CA42045 and HL38736.

REFERENCES

1. Gutniak M, Blomqvist G, Wid'en L, et al. D-[U-^{11}C]glucose uptake and metabolism in the brain of insulin-dependent diabetic subjects. *Am J Physiol* 1990;258:E805–E812.
2. Powers WJ, Dagogo-Jack S, Markham J, et al. Cerebral transport and metabolism of 1-^{11}C-D-glucose during stepped hypoglycemia. *Ann Neurol* 1995;38:599–609.
3. Hiraiwa M, Nonaka C, Abe T, et al. Reversible symmetrical white matter low attenuation in rubella encephalitis. Both in x-ray CT and ^{11}C-glucose positron emission tomography. *Neuropediatrics* 1987;18:54–56.
4. Shimizu H, Ishijima B. Diagnosis of temporal lobe epilepsy by positron emission tomography. *Folia Psychiatr Neurol Jpn* 1985;39:251–256.
5. Kishimoto H, Takazu O, Ohno S, et al. Carbon-11-glucose metabolism in manic and depressed patients. *Psychiatry Res* 1987;22:81–88.
6. Kishimoto H, Kuwahara H, Ohno S, et al. Three subtypes of chronic schizophrenia identified using ^{11}C-glucose positron emission tomography. *Psychiatry Res* 1987;21:285–292.
7. Wiesel FA, Wik G, Sjogren I, et al. Regional brain glucose metabolism in drug free schizophrenic patients and clinical correlates. *Acta Psychiatr Scand* 1987;76:628–641.
8. Wik G, Wiesel FA. Regional brain glucose metabolism: correlations to biochemical measures and anxiety in patients with schizophrenia. *Psychiatry Res* 1991;40:101–114.
9. Spence AM, Graham MM, Muzi M, et al. Feasibility of imaging pentose cycle glucose metabolism in gliomas with PET: studies in rat brain tumor models. *J Nucl Med* 1997;38:617–624.
10. Spence AM, Muzi M, Graham MM, et al. Glucose metabolism in human malignant gliomas measured quantitatively with PET, 1-[^{11}C]glucose and FDG: analysis of the FDG lumped constant. *J Nucl Med* 1997;39:440–448.
11. Ericson K, Lilja A, Bergstrom M, et al. Positron emission tomography with

([^{11}C]methyl)-L-methionine, [^{11}C]D-glucose, and [^{68}Ga]EDTA in supratentorial tumors. *J Comput Assist Tomogr* 1985;9:683–689.
12. Powers WJ. Radiation absorbed dose estimates for [1-carbon-11]-glucose in adults: the effects of hyperinsulinemia. *J Nucl Med* 1996;37:1668–1672.
13. Shiue C-Y, Wolf AP. The synthesis of 1-[C-11]-D-glucose and related compounds for the measurement of brain glucose metabolism. *J Label Comp Radiopharm* 1985;22: 171–182.
14. Dence CS, Powers WJ, Welch MJ. Improved synthesis of 1-[^{11}C]D-glucose. *Appl Radiat Isot* 1993;44:971–980.
15. Link JM, Coulter JH, Krohn KA. Remote automated synthesis of 1-[C-11]-D-glucose for patient imaging with PET [Abstract]. *J Nucl Med* 1989;30:928P.
16. Lewellen T, Kohlmyer S, Miyaoka R, et al. Investigation of the count rate performance of the General Electric advance positron emission tomograph. *IEEE Trans Nucl Sci* 1995;42:1051–1057.
17. Graham MM, Lewellen BL. High-speed automated discrete blood sampling for positron emission tomography. *J Nucl Med* 1993;34:1357–1360.
18. Rhodes CG, Wollmer P, Fazio F, Jones T. Quantitative measurement of regional extravascular lung density using positron emission and transmission tomography. *J Comput Assist Tomogr* 1981;5:783–791.
19. Cristy M, Eckerman K. Specific absorbed fractions of energy at various ages from internal photon sources. *ORNL/TM-8381 V1–V7*.Oak Ridge, TN: Oak Ridge National Laboratory; 1987.
20. Stabin MG. MIRDOSE: personal computer software for internal dose assessment in nuclear medicine. *J Nucl Med* 1996;37:538–546.
21. Snyder WS, Ford MR, Warner GG, Watson SB, eds. "S" absorbed dose per unit cumulated activity for selected radionuclides and organs. *Medical internal radiation dose committee (MIRD), pamphlet no. 11.* New York: Society of Nuclear Medicine; 1975.
22. Graham MM, Peterson LM, Link JM, et al. Fluorine-18-fluoromisonidazole radiation dosimetry in imaging studies. *J Nucl Med* 1997;38:1631–1636.
23. 1990 Recommendations of the International Commission on Radiological Protection. *ICRP publication 60.* Oxford, England: Pergamon Press; 1991.
24. Lifton JF, Welch MJ. Preparation of glucose labeled with 20-min half-lived carbon-11. *Radiation Res* 1971;45:35–40.
25. Hawkins RA, Mans AM, Davis DW, et al. Cerebral glucose use measured with [^{14}C]glucose labeled in the 1, 2, or 6 position. *Am J Physiol* 1985;248:C170–C176.
26. Mejia AA, Nakamura T, Masotoshi I, et al. Estimation of absorbed doses in humans due to intravenous administration of fluorine-18-fluorodeoxyglucose in PET studies. *J Nucl Med* 1991;32:699–706.

Placental Binding and Transfer of Radiopharmaceuticals: Technetium-99m *d*, 1-HMPAO

Azu Owunwanne, Alexander Omu, Mohan Patel, Mercy Mathew, Alia Ayesha and Sati Gopinath
Departments of Nuclear Medicine and Obstetrics and Gynecology, Faculty of Medicine, Kuwait University; and Kuwait Central Radiopharmacy, Kuwait Cancer Control Center, Kuwait

Placental binding and transfer of ^{99m}Tc *d*, 1-hexamethyl propyleneamine oxime (HMPAO) was studied in vitro using human placenta and pregnant guinea pigs. **Materials and Methods:** Five pieces of human placenta were incubated in 50 ml Earle's solution containing 1.85 MBq ^{99m}Tc *d*, 1-HMPAO. The percent binding of the tracer to the placenta per 1 ml standard solution was calculated. Pregnant guinea pigs representing first, second and third trimesters were each injected with 74 MBq ^{99m}Tc *d*, 1-HMPAO through the jugular or femoral vein after sedation was induced with pentabarbital sodium. Static images were obtained, the guinea pigs were killed, and the fetuses were removed, weighed and imaged separately. The placentas, maternal and fetal brains, lungs, livers and kidneys also were removed, and the radioactivity was assayed in a dose calibrator for each organ. The percent radioactivity in each organ was calculated. **Results:** The binding of ^{99m}Tc *d*, 1-HMPAO to human placenta ranged from 2.95% ± 1.5% to 5.82% ± 0.3% per 1 ml standard solution. Both the binding of ^{99m}Tc *d*, 1-HMPAO to guinea pig placenta and its transfer to the fetus increased with gestational age. The percent binding ranged from 0.09% ± 0.06% to 0.43% ± 0.05%, whereas that of transfer to the fetus ranged from 0.05% ± 0.03% to 2.19% ± 0.64%. Of the amount transfered to the fetus, the order of accumulation in the fetal organs was liver > blood ≫ brain > lungs > kidneys > heart. **Conclusion:** Technetium-99m *d*, 1-HMPAO binds to the placenta, and a minimal amount crosses the placental barrier and is transfered into the fetal circulation, mostly in the liver but a measurable amount is found in brain tissue.

Key Words: technetium-99m *d*, 1-hexamethyl propyleneamine oxime; placental binding; transfer; guinea pigs

J Nucl Med 1998; 39:1810–1813

Radiopharmaceuticals are administered for diagnostic and therapeutic purposes. They could be given inadvertently during pregnancy or on rare occasions, be given deliberately to save the life of either the fetus or the mother (*1–3*) and for placental localization (*4–6*). In either situation, an accurate estimate of the radiation absorbed dose to the fetus is necessary. Such a dosimetric calculation would be based on the amount of radioactivity transferred to the fetus across the placenta and/or irradiation from adjacent organs such as the urinary bladder and the placenta. For obvious ethical reasons, there are few human studies on placental binding and transfer of radiopharmaceuticals. Even in experimental animals, few studies have been reported on the transfer of radiopharmaceuticals across the placenta to the fetus (*7*). Hence, there is a need to systematically study placental transfer, biodistribution and kinetics of radiopharmaceuticals in the fetus.

In this report the binding of ^{99m}Tc *d*, 1-hexamethyl propyleneamine oxime (HMPAO) to human and guinea pig placentas and its transfer and distribution in the guinea pig fetus are described.

MATERIALS AND METHODS

In Vitro

Placental binding was studied using human placental villous tissue within 45–50 min of delivery, according to the modified method described by Smith et al. (*8*) and Guerre-Millo et al. (*9*). Five fragments each weighing approximately 0.5 g were excised from the placentas and thoroughly washed in Earle's solution (pH 7.4). The fragments were incubated in 50 ml Earle's solution equilibrated with a gas mixture of 95% oxygen and 5% carbon dioxide for 5, 10, 15, 30 or 60 min. An aliquot of 1.85 MBq (50 μCi) of the original formulation of ^{99m}Tc *d*, 1-HMPAO was added to the incubation medium. At the appropriate time interval, the fragments were blotted with tissue paper and the radioactivity was measured. A standard solution of 1.85 MBq of ^{99m}Tc *d*, 1-HMPAO diluted in 50 ml was prepared, and the radioactivity of 1 ml of it also was measured. The percent binding per radioactivity in the 1-ml standard solution was calculated. The above procedure was repeated four times for each incubation time period. A graph of

Received Aug. 5, 1997; revision accepted Jan. 14, 1998.
For correspondence or reprints contact: Azu Owunwanne, PhD, Department of Nuclear Medicine, Faculty of Medicine, P.O. Box 24923, Safat 13110, Kuwait.